

RESEARCH PAPER

Design of a dual-wideband monopole antenna by artificial bee colony algorithm for UMTS, WLAN, and WiMAX applications

DENIZ USTUN¹ AND ALI AKDAGLI²

In this study, a dual-wideband monopole antenna has been designed and developed for the universal mobile telecommunications system (UMTS), wireless local area network (WLAN), and worldwide interoperability for microwave access (WiMAX) applications. A novel approach integrating artificial bee colony (ABC) with the HyperLynx® 3D electromagnetic platform based on the method of moments has been employed to calculate the design parameters of the monopole antenna performance for the respective target frequencies and return loss. The proposed dual-wideband antenna operates in the dual-frequency ranges of 1.69–3.99 and 4.75–6.22 GHz applicable for the UMTS, WLAN, and WiMAX applications and it is fabricated on the flame resistant-4 substrate plate of $42 \times 51 \times 1.6 \text{ mm}^3$. The performance of the presented monopole antenna is analyzed in terms of gain, radiation pattern, and s -parameter. The input reflection coefficient (S_{11}) parameter and radiation pattern of the antenna are verified through the measurements. The measured values of the antenna parameters are found to match well within tolerable limits with the simulation results. The results illustrate that the presented dual-wideband monopole antenna obtained by using the ABC algorithm exhibits better performance in point of operating bands and s -parameter as compared with the multi-band antennas previously published in the literature.

Keywords: Antenna design, Modeling and measurements, Modeling, Simulation and characterizations of devices and circuits, Artificial bee colony algorithm, Dual-wideband, UMTS, WLAN, WiMAX

Received 12 December 2015; Revised 13 November 2016; Accepted 21 November 2016; first published online 21 December 2016

1. INTRODUCTION

With the development of technologies, communication devices need the antenna that operates at multi-band applications. Therefore, the basic aim of the antenna designers is to develop an antenna that integrates several wireless communication applications operating at different frequency bands into the single device. The wireless network technologies such as universal mobile telecommunications system (UMTS), wireless local area network (WLAN), and worldwide interoperability for microwave access (WiMAX) have been widely used in wireless communication. In order to meet the requirement of such multi-band operations besides the size reduction, the microstrip antennas (MAs) and the compact MAs have been particularly preferred since their advantages such as good radiation pattern, low cost, small size, easy fabrication, and integrability with microwave devices. Numerous studies have been recently proposed to improve the MA's design having properties as small size, wideband, or multi-band [1–12]. A dual-band microstrip-fed patch antenna with a pair of

inverted L-shaped patches for multi-band applications was presented in the literature [6]. The presented antenna with a simple structure has very good performance, but the size of the antenna is too big. In another work, an antenna design suggested in [10] consists of a double-sided dipole. While the antenna operates at the WLAN and WiMAX bands (2.5/3.5/5.5 GHz), it does not work below 2 GHz corresponding to UMTS application. A dual-band split-ring antenna with a near-compact design was presented, but it only operates at 2.4 and 5.2 GHz frequencies of WLAN [9]. As explained above, the antenna structures designed for wireless communication applications can be considered with their own benefits and limitation. However, it should be noted that designing a single antenna that fulfills all the demands such as wideband, compactness, and multi-band operation properties is a challenging task.

Nowadays, a variety of electromagnetic (EM) simulator software is commercially available HyperLynx® [13], which is one of the most powerful EM simulation platforms based on the methods of moment (MoM) [14] for the antenna designs. The HyperLynx® is a new version of the IE3D™ EM simulation software. Varied optimization techniques such as Powell, Genetic, and Random optimizers are available in the IE3D™ EM simulation software. The direction and bounds of the design variables in the optimization process are controlled by IE3D™ EM simulation software. However, the main disadvantage for the variables in the optimization is

¹Faculty of Tarsus Technology, Department of Software Engineering, Mersin University, 33400 Tarsus, Mersin, Turkey

²Faculty of Engineering, Department of Electrical–Electronics Engineering, Mersin University, 33343 Ciftlikkoy, Yenisehir, Mersin, Turkey

Corresponding author:

A. Akdagli

Email: aliakdagli@gmail.com

Table 1. The statistical results of 30 runs obtained by GA, PSO, DE, and ABC algorithms in [24] and Powell and Random optimizers.

No.	Function	Minmum		GA [24]	PSO [24]	DE [24]	ABC [24]	Powell	Random
1	Step	0	Mean	1.17×10^3	0	0	0	88938	66572.8
			StdDev	76.561450	0	0	0	75260.9	6448.46
2	Sphere	0	Mean	1.11×10^3	0	0	0	0	64762.5
			StdDev	74.214474	0	0	0	0	5539.96
3	Penalized2	0	Mean	125.0613	0.00767535	0.0021975	0	0.00195899	1.03E + 09
			StdDev	12.001204	0.016288	0.004395	0	0.00443737	1.69E + 08
4	Penalized	0	Mean	13.3772	0.0207338	0	0	0.0839808	5.27E + 08
			StdDev	1.448726	0.041468	0	0	0.164237	9.17E + 07
5	Ackley	0	Mean	14.67178	0.16462236	0	0	19.4769	20.589
			StdDev	0.178141	0.493867	0	0	0.1366	0.1655
6	Griewank	0	Mean	10.63346	0.01739118	0.0014792	0	4.10121	583.288
			StdDev	1.161455	0.020808	0.002958	0	6.37749	53.1267
7	Schwefel	-12569.5	Mean	-11593.4	-6909.1359	-10266	-12569.487	-7939.78	-2370.68
			StdDev	93.254240	457.957783	521.849292	0	861.393	471.63
8	Rastrigin	0	Mean	52.92259	43.9771369	11.716728	0	255.637	430.589
			StdDev	4.564860	11.728676	2.538172	0	45.831	20.5459
9	Dixon-price	0	Mean	1.22×10^3	0.66666667	0.66666667	0	3.60796	1.74E + 06
			StdDev	2.66×10^2	1×10^{-8}	1E-09	0	10.5965	3.92E + 04
10	Rosenbrock	0	Mean	1.96×10^5	15.088617	18.203938	0.0887707	73.5318	2.36E + 08
			StdDev	3.85×10^4	24.170196	5.036187	0.077390	179.31	4.02E + 07

Min., minimum values, Mean, mean of the best values, StdDev, standard deviation of the best values.

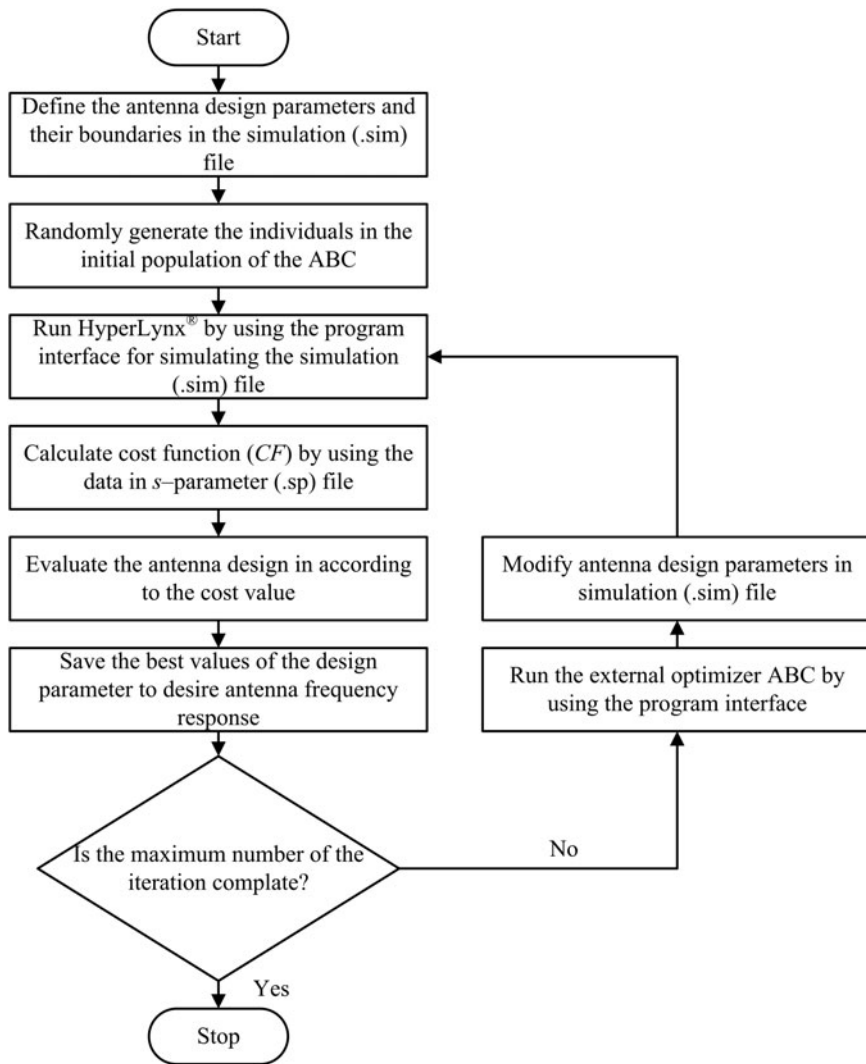


Fig. 1. Flowchart of the optimization technique for proposed the antenna design.

limited at a fixed rate of connection with each other. In the IE3DTM software, more complex relationships between the optimization variables cannot be adjusted and optimization process may induce an overlap problem. [15]. Hence, the design of antenna having slots with the complex structure cannot be carried out using the optimizer available in the HyperLynx[®].

The optimization methods based on the artificial intelligence (AI) have taken much attention in recent years because of providing fast, accurate, and flexible solutions in designing, simulation, and optimization problems at microwave frequencies. As Jin and Rahmat-Samii [16] studied in their work that the multi-wideband patch antenna was performed by using parallel particle swarm optimization (PSO) together with the finite-difference time-domain (FDTD) algorithm, while the PSO algorithm was utilized to compute a rectangular MA's length and width [17]. The genetic algorithm (GA) was used to determine the optimum feed position of the probe-feed MA [18]. The broadband patch antenna was designed by using the differential evolution (DE) algorithm and MoM [19]. A new modified planar antenna with meander lines and loads for passive RFID (radio-frequency identification) tag application at ultra-high-frequency (UHF)

band was designed. The artificial bee colony (ABC) algorithm in conjunction with other commercial EM simulation software named FEKO was used, and while the size of the antenna was minimized, the antenna gain was maximized [20]. In another study, modified spiral antennas with meander lines and loads for passive UHF tags were designed and optimized by using a Gbest-guided ABC that improved exploitation capability [21].

In the present work, the dual-wideband monopole antenna operable in the bands of UMTS, WLAN, and WiMAX applications has been designed by using a new integrated modality that consists of the ABC algorithm [22–25] and HyperLynx[®] based on MoM. The ABC algorithm is one of the most widely used optimization methods based on AI technique that can be used to find approximate solutions to extremely difficult numerical problems [22–25].

The paper is organized as follows. In Section II, the ABC is briefly presented. Section III describes the antenna design procedure stage by stage. Section IV presents the processes of prototyping the proposed antenna. The performance of the proposed antenna is given in Section V. Finally, the conclusions are given in Section VI.

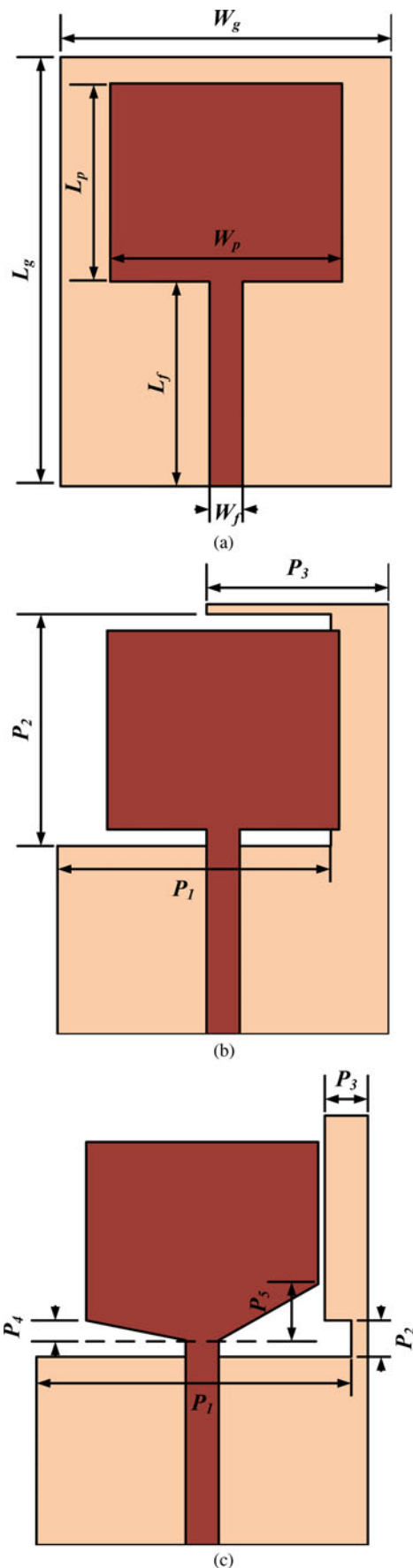


Fig. 2. Geometries of the antenna obtained by using the ABC algorithm in each design stage: (a) stage 0, (b) stage 1, (c) stage 2.

II. ABC ALGORITHM

The ABC algorithm based on swarm intelligence is an optimization technique inspired from the foraging behavior of honey bees [22–25]. The ABC consists of three different bees groups called employed, onlooker, and scout. In order to determine the optimal solution of the optimization problem, the bees in colony fly to search in a multi-dimensional solution space. The employed bees are appointed to particular nectar sources depending on themselves experiences. The onlooker bees determine nectar position based on observing the employed bees dance inside of the beehive and thus they tune their positions. Scout bees perform a random searching in the solution spaces to find the new nectar sources. At first, the half of the bee colony is assigned as onlooker bees and the other half is employed bees. The number of nectar sources representing the possible solution points for optimization problem around the hive is supposed to be equal employed bees and then the nectar source is exploited by the onlooker and employed bees. Thereafter, the employed bee which consumes the source of nectar transforms a scout bee to find more nectar sources once again. Initially, random points between two certain constraints in a solution space are determined for possible solutions related to the nectar source positions. The quality of the determined values regarding the quantities of the nectar is computed to measure the profitability at the first step. At onlooker bees step, the probability of the solution points is calculated and new solutions are found around the solution points having high probability. If the selected nectar position as the solution is not able to enhance after a definite value of trial limit, a new point is randomly identified as the same with the initial step by scout bees. Eventually, the nectar position giving the best solution determined so far is saved in memory. These steps consecutively continue until a specified maximum cycle number.

III. DESIGN PROCEDURE OF THE ANTENNA STAGE BY STAGE

In our dual-wideband monopole antenna design, we suggest to use the applied slot method into the patch and the ground plane to achieve the desired operating bands for applications of the UMTS, WLAN, and WiMAX in wireless communication technology. The dimensions of slot geometries are calculated by the ABC. The studies related to the ABC algorithm presented in the literature [23–25], which illustrates that the ABC algorithm has better performance than the others. Moreover, in order to evaluate the successes of the ABC algorithm, Powell and Random optimizers, the performance experiments were performed on the ten different benchmark functions taken from Karaboga study [24]. Each performance experiment for everyone benchmark function were repeated 30 times with different random seeds and the mean best values produced by the Powell and Random optimizers were recorded. The results of performance experiments given in Table 1 were compared with the performance values of the GA, PSO, DE, and ABC algorithms given in [24]. It can be clearly seen in Table 1 that the obtained optimization performance values of the ABC algorithm on ten benchmark functions are much better compared with Powell, Random optimizers, and others.

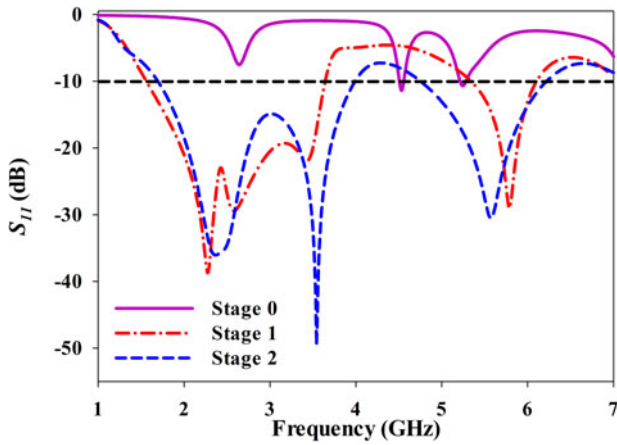


Fig. 3. Simulated S_{11} -parameter variations of the antenna design.

In the present work, an improved novel optimization method by integrating ABC algorithm with HyperLynx[®] was preferred in the design stages of the monopole antenna. The design details of the proposed antenna consist of three stages: The first stage is the analyzing process of the draft antenna by using HyperLynx[®] software. The second and third stages are a determination process of optimal antenna geometry. It includes the optimal calculation of the physical parameter's value of the slots on the patch and the ground plane by using the proposed optimization method according to specified design purposes. Furthermore, the DE and PSO

Table 2. Physical parameters (in mm) of an RMA given in stage 0.

Parameters	L_g	W_g	L_p	W_p	L_f	W_f
Values	51	42	25	30	19	3

Table 3. Lower and upper bounds (in mm) for stage 1.

Parameters	P_1	P_2	P_3
Lower bounds	0	0	0
Upper bounds	41	41	42

Table 4. Optimum values of the parameters (in mm) by using the ABC, DE and PSO algorithms for stage 1.

	Algorithms		
	ABC	DE	PSO
P_1 values	35.2	37.0	40.4
P_2 values	14.5	0.8	20.0
P_3 values	21.8	5.0	7.7

Table 5. The obtained normalized best cost values by the ABC, DE, and PSO algorithms for stage 1.

Algorithms	Normalized best cost value
ABC	0.7379
DE	0.7583
PSO	0.7946

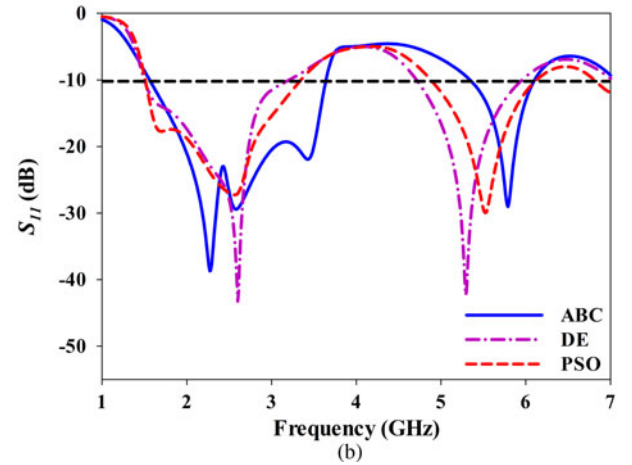
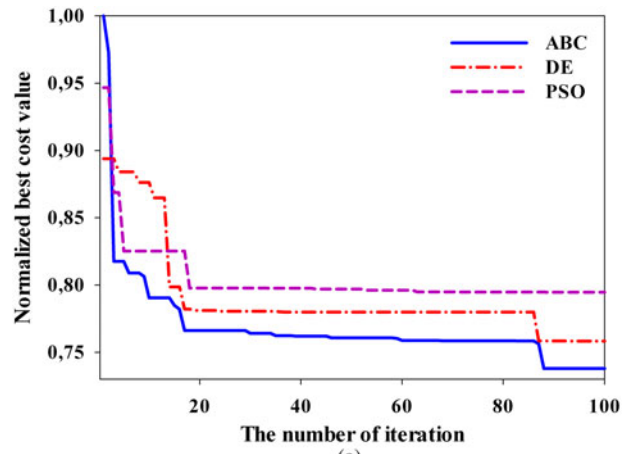


Fig. 4. Evolution curves and S_{11} graphs for the ABC, DE, and PSO algorithms in Stage 1: (a) Evolution curves, (b) S_{11} -parameters.

algorithms were also applied for the optimization of the monopole antenna design to compare with the performance of the ABC algorithm. The optimization process was performed on the personal computer having an Intel i7 processor and 16 GB memory. The antenna was designed on a volume of $42 \times 51 \times 1.6 \text{ mm}^3$ with a dielectric permittivity of 4.4 (flame resistant-4 (FR4)). In the simulations, the radiating element was supposed to 50Ω microstrip feed line with a strip width of 3 mm, which was induced by 1 V wave source. Besides, the mesh lines per wavelength ratio were set to be 20 in limit of 7 GHz. The used optimization cost functions (CFs) for the antenna design problem can include the other antenna parameters such as; pattern, gain, and polarization (as depending on the purpose of the design). However, the multi-objective CFs have several disadvantages like; increasing computer system requirements or computational time of optimal solutions for the optimization problem. In order to avoid these disadvantages, the S_{11} parameter, one of the most important factors for the antenna operating band, was used as the objective function in our antenna design. The

Table 6. Lower and upper bounds (in mm) for stage 2.

Parameters	P_1	P_2	P_3	P_4	P_5
Lower bounds	0	0	0	0	0
Upper bounds	41	41	42	15	15

Table 7. Optimum values of the parameters (in mm) by using the ABC, DE, and PSO algorithms for stage 2.

	Algorithms		
	ABC	DE	PSO
P_1 values	40.5	40.6	40.4
P_2 values	4.9	4.2	20.1
P_3 values	3.7	3.6	3.0
P_4 values	0.7	0.7	0.5
P_5 values	5.5	5.6	7.1

Table 8. The obtained normalized best cost values by the ABC, DE, and PSO algorithms for stage 2.

Algorithms	Normalized best cost value
ABC	0.5049
DE	0.5325
PSO	0.5975

simulation was carried out over the range of frequency from 1 to 7 GHz for 61 frequency points. But the CF given in equation (1) was used the chosen nine frequency points related to UMTS, WLAN, and WiMAX bands. The CF consisted of

pass and stop frequency points.

$$CF = \frac{1}{N} \sum_{n=1}^N C(f_n), \tag{1}$$

$$C(f_n) = \begin{cases} 0, & \text{if } (S_{11}^{Obtained} < S_{11}^{Desired}) \\ |S_{11}^{Desired} - S_{11}^{Obtained}|, & \text{otherwise} \end{cases}, \tag{2}$$

where C given in equation (2) is the cost terms in the CF, $n = 1, 2, \dots, N = 9$ and $f_n = \{1.9, 2.0, 2.1, 2.4, 2.5, 3.5, 5.2, 5.5, 5.8\}$

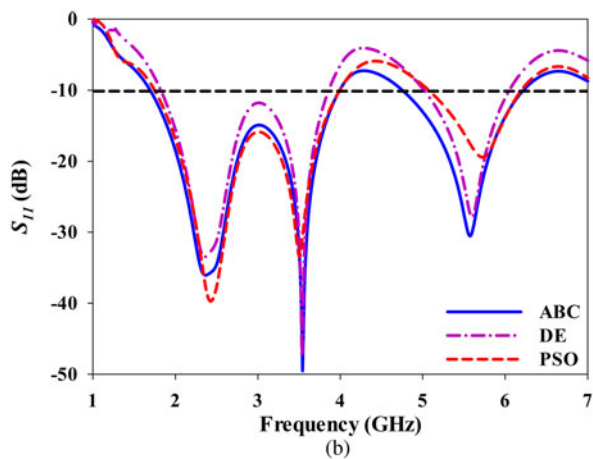
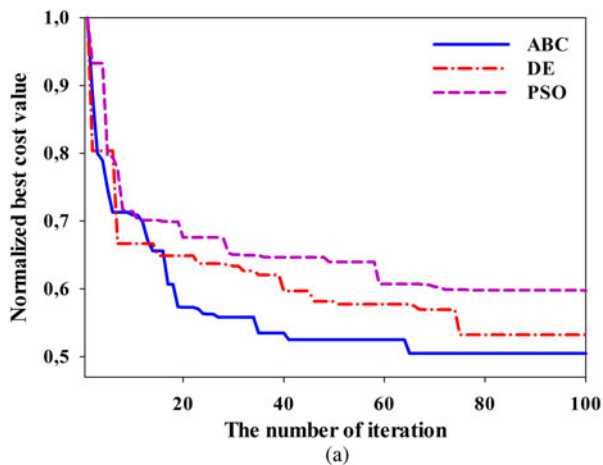
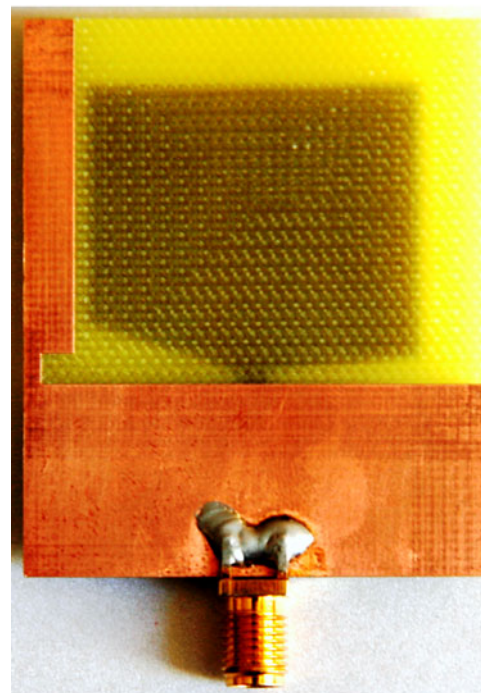


Fig. 5. Evolution curves and S_{11} graphs for the ABC, DE, and PSO algorithms in stage 2: (a) Evolution curves, (b) S_{11} -parameters.



(a)



(b)

Fig. 6. The illustration of the fabricated antenna: (a) Front view (b) Back view.

Table 9. Reported multiband antennas in the literature.

References	Size (mm ²)	Total area (mm ²)	UMTS (GHz)	WLAN (GHz)	WiMAX (GHz)
[1]	30 × 25	750	–	2.4/5.2/5.8	–
[2]	50 × 30	1500	–	2.4/5.2/5.8	–
[3]	30 × 25	750	–	–	2.5/3.5/5.5
[4]	23 × 36.5	839.5	–	2.4/5.8	2.5/3.5
[5]	20 × 38	760	–	2.4/5.8	2.5/3.5
[6]	70 × 60	4200	–	5.2/5.8	3.5/5.5
[8]	62 × 64	3720	–	5.2/5.8	3.5
[9]	14 × 15	210	–	2.4/5.2	–
[10]	50 × 50	2500	–	2.4	3.5/5.5
[11]	28 × 32	896	–	2.4/5.2	2.5/3.5
[12]	22 × 26	572	–	2.4/5.2	–
Proposed antenna	42 × 51	2142	1.9/2.1	2.4/5.2/5.8	2.5/3.5/5.5

GHz frequencies. The maximum value of $S_{11,Desired}$ is chosen as -30 dB for this study.

A brief flowchart of the proposed optimization technique is given in Fig. 1. The ABC algorithm integrating the EM program mainly used to exchange the generated simulation (.sim) and the s -parameter (.sp) data files by the HyperLynx[®]. At the first step, the ABC initial parameters called as trial, iteration numbers, and colony size are set. Then, the possible solutions representing the values of antenna design variables are randomly generated. The ABC algorithm has changed these values in the generated simulation (.sim) file. The new simulation (.sim) file is then simulated by HyperLynx[®]. The return loss results of the antenna obtained with simulation are saved in s -parameter (.sp) file. In the last step, the CF is calculated by using return loss data and it is evaluated by the ABC algorithm. The algorithm generates new sets of data called possible solutions for performing better antenna design. The data sets are being recursively improved until the number of iterations as a target.

In all of antenna design, the common optimization parameters used in each algorithm such as population size and maximum evolution numbers were. The population size was 50 and the maximum evolution number was 100. The specific parameters of the algorithms were given below:

ABC setting: The limit parameter value of the ABC was defined by using the dimension of the problem and size of the colony as given in the following equation:

$$\text{limit} = SN \times D, \tag{3}$$

where SN is the number of the employed bees or food sources, and D is the dimension of the problem.

DE setting: F which affects the differential variation between solutions is a real constant. This value is set to 0.6 in this work. The value of the crossover determining the change of the diversity of the population was selected to be 0.9 in this work.

PSO setting: φ_1 and φ_2 which are the cognitive and social constants may be used for variation of weighting between individual and population experience, respectively. In this study, these constants were both set to 1.8 and inertia weight that is the scale factor of the particle velocity, was set 0.6.

The design of the antenna is demonstrated with three main stages for the better understanding of the antenna design process. The obtained final geometry of the antenna by the

ABC algorithm in each design stage are given in Figs 2(a), 2(b), and 2(c) and the simulated S_{11} curves are illustrated in Fig. 3.

A rectangular MA has given in Fig. 2(a) as stage 0, of which psychical parameters are tabulated in Table 2, has been used as a starting antenna. As shown in Fig. 3, the starting antenna in stage 0 only operates at the frequencies of 4.5 and 5.25 GHz. The performance of stage 0 is not sufficient in terms of desired bands for UMTS, WLAN, and WiMAX applications.

In order to increase the performance of S_{11} at stage 0, the starting antenna was modified by the applied slot etching method to the antenna’s patch and the ground plane. Then to determine the proper physical parameters that have an influence on the S_{11} performance positively, many simulations were carried out. After many trials, the following physical variations (depending on $P_1, P_2, P_3, P_4,$ and P_5), which produces good results are selected to use in the optimization process. $P_1, P_2,$ and P_3 represent the variations on the ground plane, whereas P_4 and P_5 symbolize the variations on patch of the antenna. In stage 1, the parameters of variation ($P_1, P_2,$ and P_3) selected for the antenna ground plane are optimized by using the ABC, DE, and PSO algorithms to obtain the best S_{11} performance than that of stage 0. The lower and upper bounds of the parameters are listed in Table 3 and optimum parameters determined by optimization algorithms are given in Table 4. The best normalized cost values by the ABC, DE, and PSO algorithms for stage 1 are displayed in Table 5. We

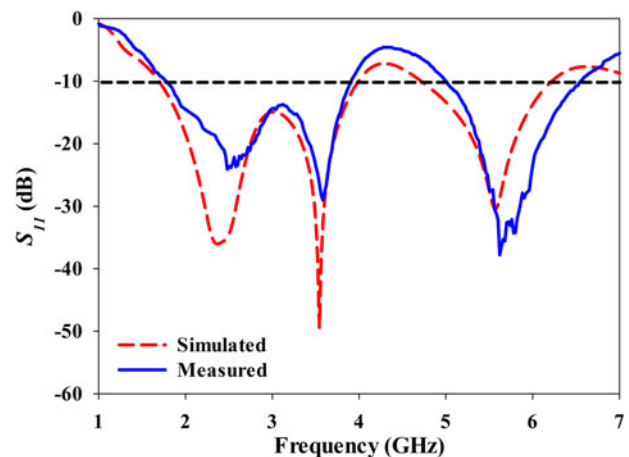


Fig. 7. Simulated and measured S_{11} -parameters of the proposed antenna.

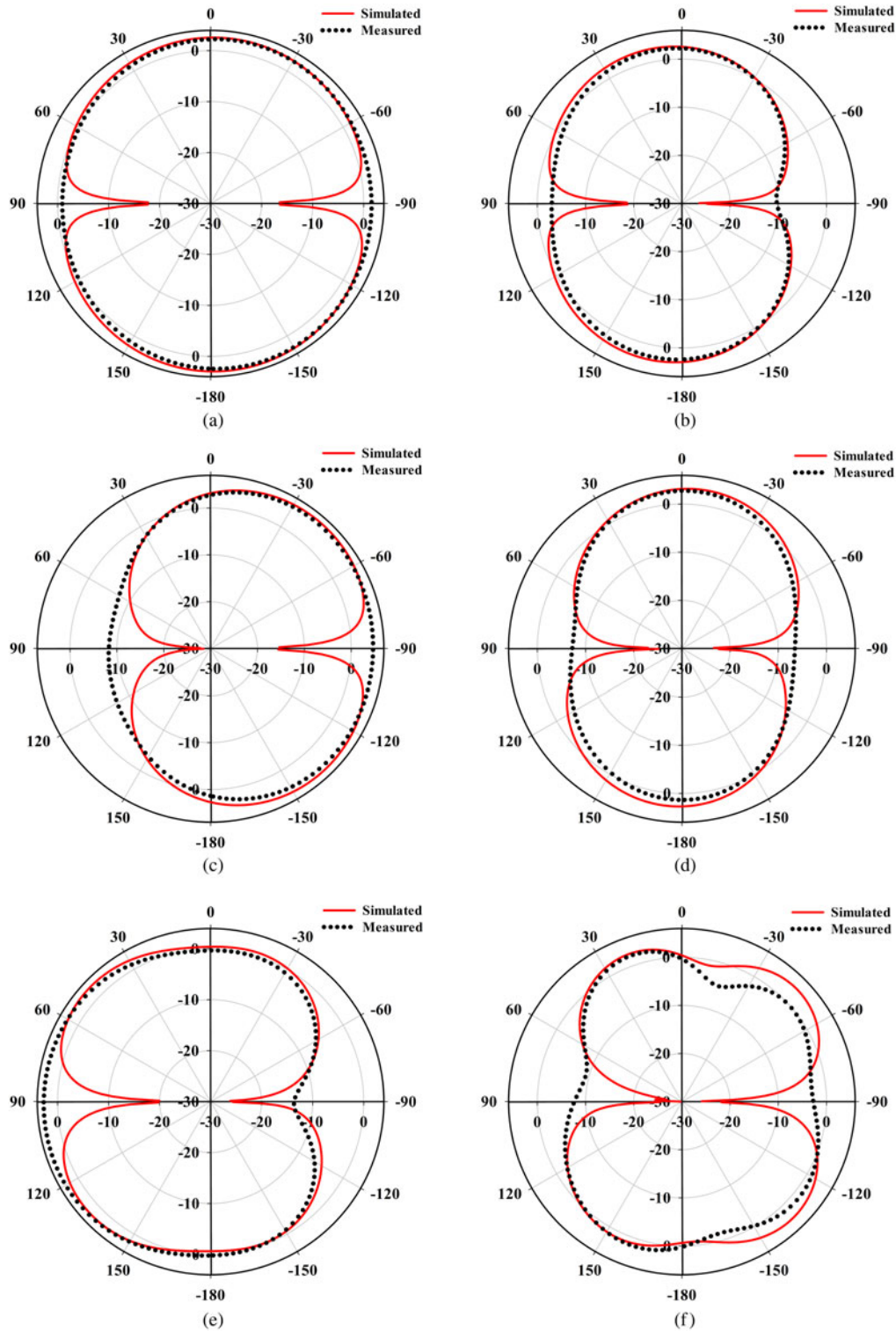


Fig. 8. Simulated and measured radiation patterns of the prototype antenna for different frequencies: (a) xz -plane for 2.4 GHz, (b) yz -plane for 2.4 GHz, (c) xz -plane for 3.5 GHz, (d) yz -plane for 3.5 GHz, (e) xz -plane for 5.5 GHz, (f) yz -plane for 5.5 GHz.

can see that the best normalized cost value of the ABC algorithm for stage 1 is smaller than the DE and PSO algorithms. The convergence graphs of all the optimization algorithms are depicted in Fig. 4(a). The convergence rate of the ABC is the faster than the other. It is clearly observed from Fig. 4(b) that a major improvement in the operating frequency bands of the monopole antenna is obtained through the optimization

methods. As seen from the values of S_{11} given in Fig. 4(b) that the operating bands of the designed antenna by using the DE and PSO algorithms cover all of the operating frequencies mentioned above for the WLAN and UMTS. But the desired operating frequency (3.5 GHz) for WiMAX application is not in the operation bands of the antenna designed. The bandwidths ($S_{11} < -10$ dB) of the design antenna by

the ABC algorithm for the first operating band is 1.56–3.64 GHz. Also, The frequency range of the second operating band is 5.34–6.10 GHz. Additionally, the design antenna by ABC includes the desired bandwidth for WiMAX operation in 3.5 GHz band. Even so, the second operating band of the antenna is insufficient. It is well known that the slots etched into the patch of the antenna can be created the positive effect of the S_{11} characteristics. Hence, the final antenna geometry in stage 2 is formed by cutting symmetrically from the bottom side of the patch and two new parameters are added to the old parameters. The parameters ($P_1, P_2, P_3, P_4,$ and P_5) determined in stage 2 are then optimized. The lower and upper bounds of the parameters are displayed in Table 6 and parameter optimum values using algorithms are shown in Table 7. The achieved normalized best cost values by the ABC, DE and PSO are given in Table 8. It can be seen that the normalized best cost value of the ABC algorithm is smaller than the DE and PSO. The convergence graphs of all the optimization algorithms are illustrated in Fig. 5(a). The ABC convergence rate is faster than the DE and PSO algorithms. As shown from Fig. 5(b) that a deeper and broadened frequency range according to the first band has been attained with last modification for all optimization algorithms used in the present work. Besides, the second band was both broadened and the shifting to upper frequencies for the ABC and DE algorithms. For the antenna designed by the proposed optimization method, the impedance bandwidths of the first and second operating bands attained are 2.30 (1.69–3.99) and 1.47 GHz (4.75–6.22 GHz), respectively. The simulation results are clearly shown that the operation bands of the final antenna design cover the above-mentioned all of operating bands of UMTS, WLAN, and WiMAX.

IV. PROTOTYPING THE PROPOSED ANTENNA DESIGN

The patch element and ground plane are fabricated on the FR4 printed circuit boards (PCB). The FR4 substrates having an epoxy glass are the material of choice for most microwave applications since it is very low cost and has good mechanical properties [26, 27]. The FR4 material is widely used as a substrate in most of the microwave antenna and filter designs. In the presented design, an FR4 material having a thickness of

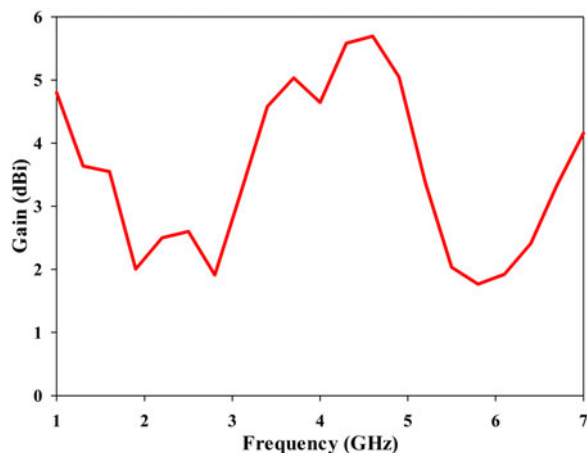


Fig. 9. The peak gain curve of the proposed antenna.

1.6 mm, dielectric permittivity of 4.4, copper foil thickness of 0.35 mm, and a tangent loss of 0.02 was used. The strip line and slot structures on the top and the bottom planes were given shape by using LPKF ProtoMat E33 compact circuit board plotter device. In the design, one-feed point with linear polarization was used. The S_{11} -parameter of the design antenna was measured by means of an Agilent E5071B ENA Series RF network analyzer.

The final antenna prototype illustrated in Fig. 6 has been successfully realized according to the dimensions in Table 7 calculated by the ABC. The measured and simulated s -parameter plots are comparatively given in Fig. 7. It is noted that the some differences between the results of simulation and measurement can be depended on the variations of the geometry, thicknesses, and permittivity of substrate, mismatch of feeding cables and copper cladding in the fabrication process.

The results show that the designed antenna operates over the two distinct operating bands. It illustrates a maximum measurement return loss at 2.48, 3.56, and 5.62 GHz are -24.07 , -28.12 , and -37.78 dB, respectively. The lower bandwidth of 2.12 GHz (< -10 dB) ranges from 1.78 to 3.90 GHz, while the upper band (bandwidth 1.54 GHz) ranges from 5.00 to 6.54 GHz. Moreover, the operating bands of the presented antenna significantly are enhanced by increasing the size value of the antenna via loading the slots. The reported studies for the multiband application in the literature are tabulated in Table 9. Small antennas are mostly useful where compactness is compulsory. However, these antennas have not got the property of the wideband. Although the similar antennas have compact properties, the bands of these antennas do not cover some of the operating bands of WLAN and WiMAX applications [1–5, 9, 11, 12]. Furthermore, the presented larger antennas in the literature [6, 8, 10], the measured bands of the WLAN and WiMAX have weaker values than the presented monopole antenna in this study. Moreover, the operating band of the proposed antenna covers the most of the WLAN and WiMAX applications. Further, it operates in the UMTS application band ranges of 1.9 and 2.1 GHz. All the results illustrate that the presented antenna configuration is a good candidate for the UMTS, WLAN, and WiMAX applications.

V. PERFORMANCE ANALYSIS OF THE PROPOSED ANTENNA

The radiation pattern of the prototype antenna is measured when the port is excited with a 50Ω load in an anechoic chamber. The measured and simulated radiation patterns of the proposed antenna for three frequencies of 2.4, 3.5, and 5.5 GHz are given in Fig. 8. The measured radiation patterns of the antenna are in good agreement with the results of the simulation. Additionally, they are nearly stable for the entire bands of the operation and the radiation patterns generally show the omnidirectional behavior for most of frequencies at the operating frequency bands. The gain curve against frequency of the antenna is illustrated in Fig. 9. The peak gain for frequencies between 1.78 and 3.90 GHz is 5.03 dBi and the value of the gain decreases in the interval of 5.00–6.54 GHz. Moreover, the peak gain is 1.94 dBi for the second operating band.

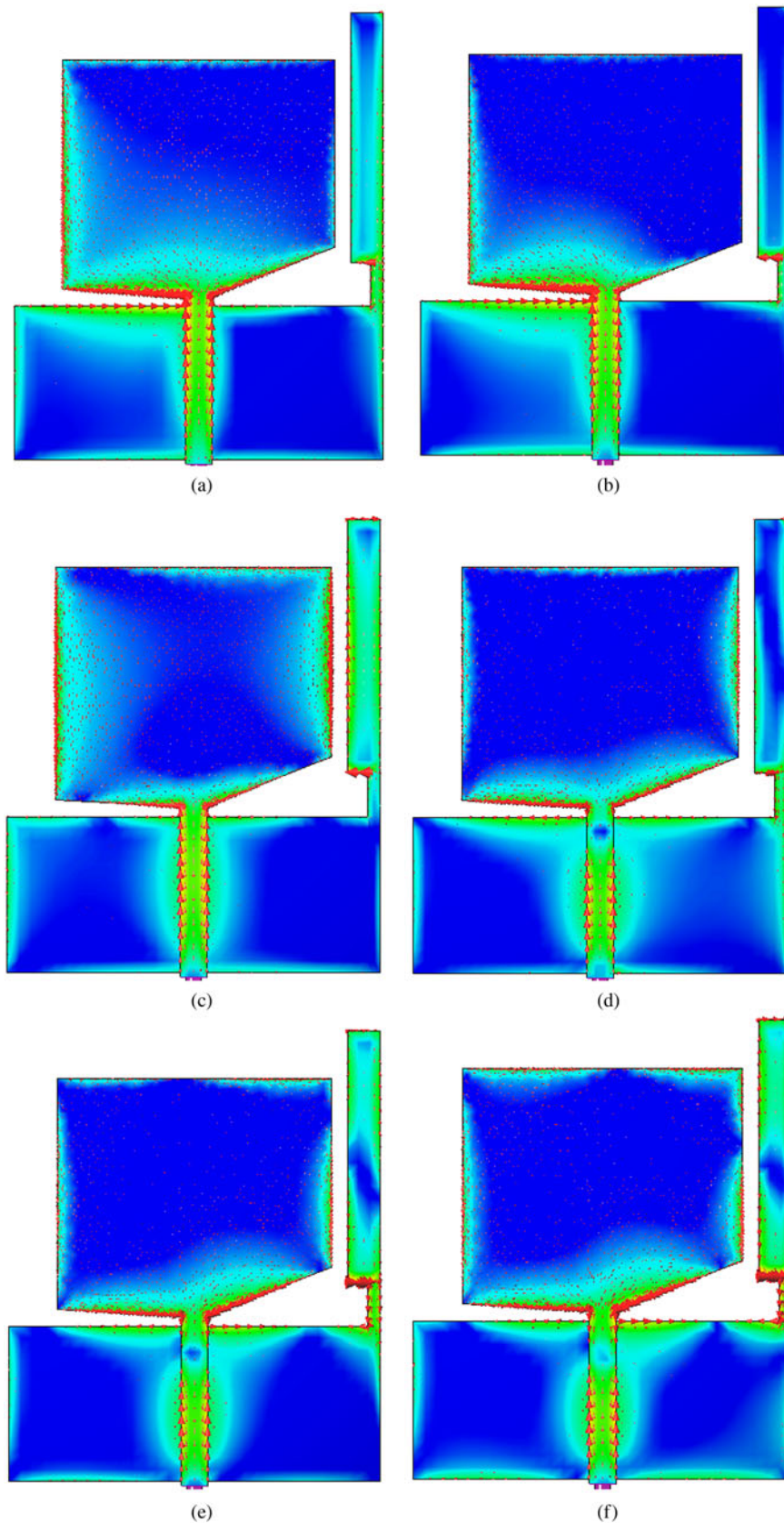


Fig. 10. Distributions of surface current: (a) 2.0 GHz, (b) 2.4 GHz, (c) 3.5 GHz, (d) 5.2 GHz, (e) 5.5 GHz, (f) 5.8 GHz.

To research the underlying current mechanism of the presented antenna, the simulated surface current distribution at the frequency points of 2.0, 2.4, 3.5, 5.2, 5.5, and 5.8 GHz

are given in Fig. 10. The surface currents are intensively concentrated along with the left bottom edge of the patch as shown in Figs 10(a) and 10(b) for 2.0 and 2.4 GHz bands,

respectively. Figure 10(c) indicates the simulated distributions of current at 3.5 GHz. It is obviously seen that the strong resonant currents flow along both sides of the patch to yield the middle resonance and the distributions of current are mainly around the strip at the right of the ground plane for 3.5 GHz band. In Fig. 10(d), the current distributions at 5.2 GHz are intensively accumulated along with the left and right bottom edges of the patch. Figures 10(e) and 10(f) show the distributions of current at 5.5 and 5.8 GHz, respectively. Obviously, the upper resonant mode is mainly collected by the bottom of the patch and right ground strip.

VI. CONCLUSIONS

In this paper, a new dual-wideband monopole antenna with simulated and measured results is clearly presented for UMTS, WLAN, and WiMAX applications. In order to achieve the required bands of the above-mentioned applications, the slots are opened into the patch and ground planes of the antenna and then the geometry of the slots is optimized by using the proposed technique based on the ABC, DE, and PSO algorithms integrated with MoM. The normalized best cost values of the ABC algorithm for the antenna design stages 1 and 2 are smaller than the DE and PSO algorithms. The ABC algorithm is seen to have a faster convergence rate than the DE and PSO algorithms. Furthermore, the combination of the slots leads to better impedance matching and creation of wide band. The proposed antenna has the capable of producing two distinct bands with $S_{11} < -10$ dB. The operating bands were about 2.12 (1.78–3.90) and 1.54 GHz (5.00–6.54 GHz). The peak gains for first and second operating bands are 5.03 and 1.94 dBi, respectively. Moreover, the proposed antenna shows nearly omnidirectional radiation behavior at the entire operating bands. All these qualities of the presented antenna make it a suitable candidate for UMTS, WLAN, and WiMAX applications.

ACKNOWLEDGEMENTS

The authors were grateful to Dr. Abdurrahim Toktas for their precious help and performing antenna simulations through the HyperLynx® 3D EM platform in Karamanoglu Mehmetbey University.

REFERENCES

- [1] Liu, W.C.; Wu, C.M.; Chu, N.C.: A compact CPW-fed slotted patch antenna for dual-band operation. *IEEE Antennas Wireless Propag. Lett.*, **9** (2010), 110–113.
- [2] Huang, C.Y.; Yu, E.Z.: A slot-monopole antenna for dual-band WLAN applications. *IEEE Antennas Wireless Propag. Lett.*, **10** (2011), 500–502.
- [3] Lu, J.H.; Huang, B.J.: Planar multi-band monopole antenna with L-shaped parasitic strip for WiMAX application. *Electron. Lett.*, **46** (2010), 671–672.
- [4] Liu, P.; Zou, Y.; Xie, B.; Liu, X.; Sun, B.: Compact CPW-fed tri-band printed antenna with meandering split-ring slot for WLAN/WiMAX applications. *IEEE Antennas Wireless Propag. Lett.*, **11** (2012), 1242–1244.
- [5] Iddi, H.U.; Kamaruddin, M.R.; Rahman, T.A.; Abdulrahman, Y.A.; Khaliq, M.; Jamlos, M.F.: triple-band CPW-fed planar monopole antenna for WLAN/WiMAX application. *Microw. Opt. Technol. Lett.*, **55** (2013), 2209–2214.
- [6] Kaur, J.; Khanna, R.: Development of dual-band microstrip patch antenna for WLAN/MIMO/WiMAX/AMSAT/WAVE applications. *Microw. Opt. Technol. Lett.*, **56** (2014), 988–993.
- [7] Kaur, J.; Khanna, R.; Kartikeyan, M.: Novel dual-band multistrip monopole antenna with defected ground structure for WLAN/IMT/BLUETOOTH/WIMAX applications. *Int. J. Microw. Wireless Technol.*, **6** (2013), 93–100.
- [8] Malekpoor, H.; Jam, S.: Design of multi-band asymmetric patch antenna for wireless applications. *Microw. Opt. Technol. Lett.*, **55** (2013), 730–734.
- [9] Basaran, S.C.; Erdemli, Y.E.: Dual-band split-ring antenna design for WLAN applications. *Turk. J. Electr. Eng. Comp. Sci.*, **16** (2008), 78–86.
- [10] Yuan, Z.X.; Yin, Y.Z.; Ding, Y.; Li, B.; Xie, J.J.: Multiband printed and double-sided dipole antenna for WLAN/WiMAX applications. *Microw. Opt. Technol. Lett.*, **54** (2012), 1019–1022.
- [11] Hu, W.; Yin, Y.Z.; Fei, P.; Yang, X.: Compact triband square-slot antenna with symmetrical L-strips for WLAN/WiMAX applications. *IEEE Antennas Wireless Propag. Lett.*, **10** (2011), 462–465.
- [12] Basaran, S.C.: Compact dual-band split-ring antenna for 2.4/5.2 GHz WLAN applications. *Turk. J. Electr. Eng. Comput. Sci.*, **20** (2012), 347–352.
- [13] HyperLynx® 3D EM. Version 15. Mentor Graphics Corporation, Wilsonville, OR.
- [14] Harrington, R.F.: *Field Computation by Moment Methods*, IEEE Press, Piscataway, NJ, 1993.
- [15] Liu, X.F.; Jiao, Y.C.; Zhang, F.S.; Chen, Y.B.: Design of a low-profile modified U-slot microstrip antenna using PSO based On IE3D. *Microw. Opt. Technol. Lett.*, **49** (2007), 1111–1114.
- [16] Jin, N.B.; Rahmat-Samii, Y.: Parallel particle swarm optimization and finite difference time domain algorithm for multiband and wideband patch antenna designs. *IEEE Trans. Antennas Propag.*, **53** (2005), 3459–3468.
- [17] Yilmaz, A.E.; Kuzuoglu, M.: Calculation of optimized parameters of rectangular microstrip patch antenna using particle swarm optimization. *Microw. Opt. Technol. Lett.*, **49** (2007), 2905–2907.
- [18] Namkung, J.; Hines, E.L.; Green, R.J.; Leeson, M.S.: Probe-feed microstrip antenna feed point optimization using a genetic algorithm and the method of moments. *Microw. Opt. Technol. Lett.*, **49** (2007), 325–329.
- [19] Zhang, L.; Cui, Z.; Jiao, Y.C.; Zhang, F.S.: Broadband patch antenna design using differential evolution algorithm. *Microw. Opt. Technol. Lett.*, **51** (2009), 1692–1695.
- [20] Goudos, S.K.; Siakavara, K.; Sahalos, J.N.: Modified spiral RFID tag antenna optimal design using artificial bee colony optimization, in *Proc. 43rd European Microwave Conf.*, Nuremberg, Germany, 2013, 1255–1258.
- [21] Goudos, S.K.; Siakavara, K.; Sahalos, J.N.: Optimizing meandered spiral antenna for RFID tags using Gbest-guided artificial bee colony algorithm, in the *8th European Conf. on Antennas and Propagation (EuCAP 2014)*, Hague, The Netherlands, 2014, 2962–2965.
- [22] Karaboga, D.; Akay, B.: Artificial bee colony (ABC), harmony search and bees algorithms on numerical function optimization, in *Iproms 2009 Innovative Production Machines and Systems Virtual Conf.*, Cardiff, UK, 2009, 417–422.

- [23] Karaboga, D.; Basturk, B.: A powerful and efficient algorithm for numerical function optimization: artificial bee colony (ABC) algorithm. *J. Glob. Optim.*, **39** (2007), 459–471.
- [24] Karaboga, D.; Akay, B.: A comparative study of artificial bee colony algorithm. *Appl. Math. Comput.*, **214** (2009), 108–132.
- [25] Karaboga, D.; Basturk, B.: On the performance of artificial bee colony. *Appl. Soft. Comput.*, **8** (2008), 687–697.
- [26] Yamacli, S.; Ozdemir, C.; Akdagli, A.: A method for determining the dielectric constant of microwave PCB substrates. *Int. J. Infrared Millim.*, **29** (2008), 207–216.
- [27] Khan, A.; Nema, R.: Analysis of five different dielectric substrates on microstrip patch antenna. *Int. J. Comput. Appl.*, **55** (2012), 6–12.



Deniz Ustun was born in 1976. He received his B.Sc. degree in the Department of Computer Science Engineering from Istanbul University, Turkey in 2001. He obtained his M.Sc. degree in Electrical–Electronics Engineering from Mersin University, Turkey, in 2009. Since 2010, he has been working toward the Ph.D. degree at the same department.

He has been working as a Lecturer in the Department of Software Engineering, Mersin University since 3 years. His current research interests are artificial neural network, computational electromagnetic, evolutionary optimization methods (differential evolution, particle swarm

optimization, artificial bee colony, and hybrid algorithms), computer modeling and simulation (microstrip antennas, computational electromagnetic), and applications of optimization algorithms to an electromagnetic problem such as radiation, resonance, and bandwidth.



Ali Akdagli received his B.S., M.S., and Ph.D. degrees in Electronic Engineering from Erciyes University, Kayseri, in 1995, 1997, and 2002, respectively. From 2003 to 2006, he was an Assistant Professor in the Electronic Engineering Department at Erciyes University. He joined the same department at Mersin University, where he currently works

as a Professor. He has published more than 90 papers in journals and conference proceedings. His current research interests include evolutionary optimization techniques (genetic algorithm, ant colony optimization, differential evolution, particle swarm optimization, and artificial bee colony algorithms), artificial neural networks and their applications to electromagnetic, wireless communication systems, microwave circuits, microstrip antennas, and antenna pattern synthesis problems. He is an editorial board member of “Recent Patents on Electrical Engineering”, “International Journal of Computers”, and “Journal of Computational Engineering”.